



Classic Herb Pair Scutellaria Barbata and Hedyotis Diffusa for Breast Cancer: Potential Mechanism with Method of Network Pharmacology

TingTing Ma^{ab}, GanLin Zhang^a, BingXue Li^{ab}, CunFang Dai^a, XiaoMin Wang^{a*}

^a Oncology Department, Beijing Hospital of Traditional Chinese Medicine, Capital Medical University, No.23, Back Road of Art Gallery, Dongcheng District, Beijing 100010, China.

^b Beijing University of Chinese Medicine, No. 11 East North Third Ring Road, Chaoyang District, Beijing, 100029, China.

Abstract

Background: Although with diverse treatments and relative long survival times, the recurrences and metastasis are still prevalence after regular therapies, making breast cancer the most serious threatening disease for women all over the world. As empirical medicine, TCM are frequently and widely used for efficacy enhancing and toxicity reducing in the treatment of cancer. The combination using of scutellaria barbata and hedyotis diffusa is a classic herb pair SH prescribed by many famous Chinese oncologists. With the help of SH after western medicine therapeutics, recurrence reduction, metastasis reduction and even the decline of tumour markers can be observed in clinical cases. However, the underlying mechanism of SH for breast cancer is unclear. TCM network pharmacology approach provides a new research paradigm for translating TCM from an experience-based medicine to an evidence-based medicine system, potential mechanisms of TCM may be revealed with network pharmacology method. Based on clinical effectiveness observations, we did *in vitro* experiments and mined the network pharmacology of SH to analyse the role of SH and its potential mechanisms.

Methods: On the basis of TCM decoction process, lyophilized powder of SH is prepared. Both human-derived and mouse-derived breast cancer cells were used to evaluate the efficacy of SH. The active ingredients in SH lyophilized powder were identified by high performance liquid chromatography (HPLC). Cell proliferation test and cell scratch test were used to assess the effect of SH on breast cancer cells proliferation and migration. Then corresponding potential target genes were extracted from Swiss Target Prediction and SEA databases. For breast cancer, disease target genes were searched with "breast cancer" as keywords from databases Therapeutic Target Disease, Drug bank, Disease Gene NET and Genetic Association Database. In addition, with intersection genes of SH and breast cancer were mapped, the Protein-Protein Internetwork (PPI) network of shared genes was constructed with String Database. In the last, Gene Oncology (GO) and Kyoto Encyclopaedia of Genes and Genomes (KEGG) functional annotation clusters were acquired from String database and presented as top 30 pathways.

Results: SH lyophilized powder inhibited the proliferation and migration of both human-derived and mouse-derived breast cancer cells. Further, 75 active ingredients and 180 target genes were extracted for SH, simultaneously, 1305 related genes were extracted for breast cancer. Then 86 intersection genes of SH and breast cancer were mapped. With all the visualization process, combining the basis of physiology and pathology, MicroRNAs in cancer, steroid hormone biosynthesis, serotonergic synapse, VEGF signalling pathway, EGFR tyrosine kinase inhibitor resistance and NF-Kappa B signalling pathway et al were detected in the Top 30 KEGG clusters list from the intersection genes of SH and breast cancer, indicating possible effective mechanisms of SH for breast cancer.

Conclusion: SH can inhibit breast cancer with several potential mechanisms which provide more evidence for clinic. Further experiments and signal pathways analysis are needed to better understand SH.

Keywords:

Herb pair;
Scutellaria barbata;
Hedyotis diffus;
Breast cancer;
Network pharmacology.

* CONTACT: Xiao-Min Wang: wangxiaomin_bhtcm@126.com. Gan-Lin Zhang: kalinezhang@163.com.

Introduction

Breast cancer has always been the most serious threatening disease for women all over the world. Recurrence and metastasis are prevalence after those regular therapies such as operation, radiotherapy and chemotherapy, which usually lead to a decreased quality of life as well. As an empirical medicine, traditional Chinese Medicine (TCM) is frequently and widely used for efficacy enhancing and toxicity reducing in the treatment of cancer in China. With the ever-increasing acceptance of complementary and alternative medicine in the world, Chinese herbal medicine (CHM) appeared in many cancer centres in Asia, Africa and some western countries^[1-3]

In the TCM theory, the pathological bases of breast cancer are Qi Deficiency, Blood Stasis and Toxin, and the corresponding treating principle are Tonifying Qi, Invigorating Blood Circulation and Detoxification. The combination using of *scutellaria barbata* and *hedyotis diffusa* (SH) is a classic herb pair in the detoxification method and frequently used by many Chinese oncologists. There was a study^[4] claimed that *Hedyotis diffusa* plus *Scutellaria barbata* was the core treatment of CHM used to treat breast cancer in Taiwan. However, despite its curative effects, TCM has been trapped in the position of empirical drug use for its complex ingredients.

Network pharmacology approach, first proposed by Andrew L Hopkins in 2008^[5], provides a new research paradigm for translating TCM from an experience-based medicine to an evidence-based medicine system. Active components, potential targets, biological processes and pathways of TCM may be revealed with network pharmacology method^[6]. Chinese herbal formulae may influence many targets with many kinds of herbs, the use of TCM may become an advantage for aiming to multiple targets with multiple ingredients if we can explain the mechanisms more clear and logic. Wang et al have explored multiple targets of *Ai Du Qing* for breast cancer^[7], as well as some other Chinese Medicine for different diseases^[8-10].

In the present study, the efficacy of SH on breast cancer were analysed by experiments *in vitro* and the potential mechanisms were explored by network pharmacology.

Materials and Methods

The study mainly included three procedural modules: a. form evolution and ingredient identification of SH pair, b. clinical experiences and efficacy evaluation of cell experiments, c. network construction and pathways enrichment based on target genes fishing and mapping. (Figure1)

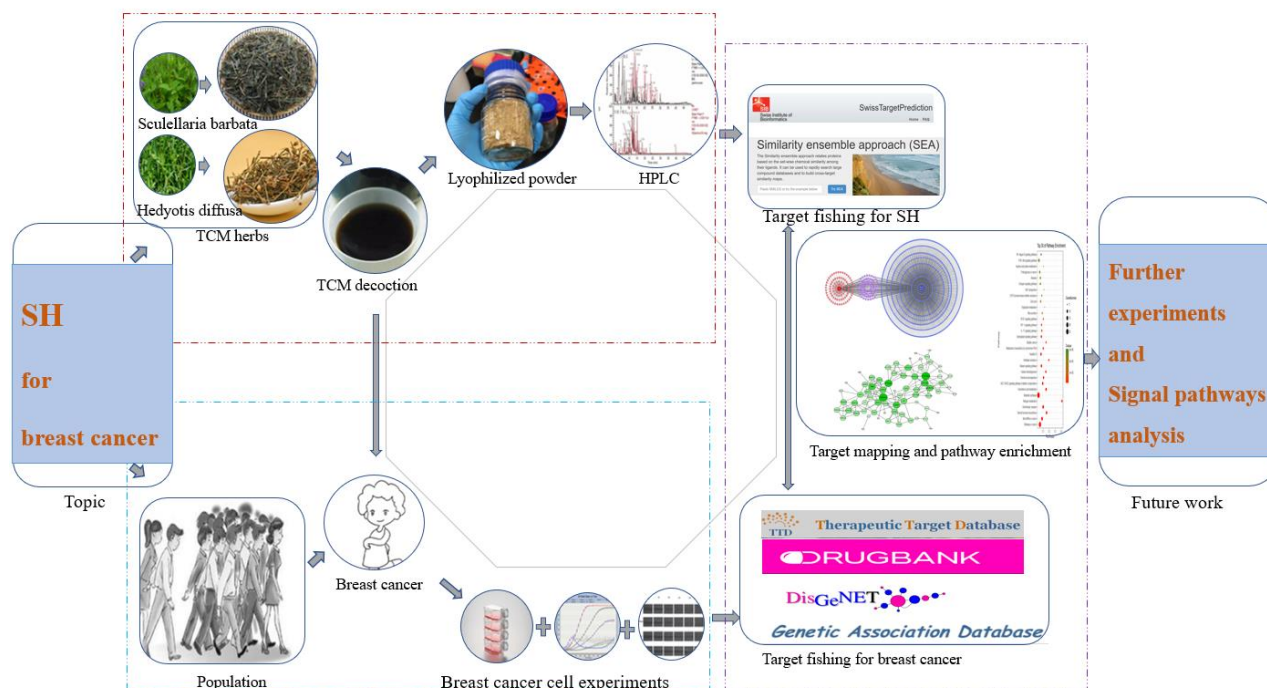


Figure 1 The framework for SH on breast cancer based on network pharmacology

SH is a herb pair with equal weight of *Scutellaria barbata* and *Hedyotis diffusa*, both of which were purchased from Beijing Hospital of Traditional Chinese Medicine, Capital Medical University. SH lyophilized powder was acquired by Vacuum cryogenic freeze dryer (Epsilon 2-4LSC, Chris, German). Mass spectrometry analysis was analysed by LTQ-Oribitrap XL linear ion trap tandem electrostatic field trap mass spectrometer: equipped with thermal spray ion source (HESI), Xcalibur 2.1 chemical workstation (Thermo Scientific company, USA); Dionex Ultimate 3000 UHPLC Plus Focused ultra high liquid chromatography system (Thermo Scientific company, USA). Millipore Synergy UV Ultra

Pure Water Machine (Millipore Company, USA); Sartorius BT 25S 1/10000 Electronic Analysis Balance (Beijing Sedoris Instrument Co., Ltd.,China); Ultrasound Cleaner (Beijing Zhongsheng Technology Co., Ltd., China); 0.22 μm Microporous Filtration Membrane (Tianjin Jinteng Experimental Equipment Co., Ltd.,China); Formic Acid and Methanol (Fisher Company, USA). Apigenin, scopolamine and caffeic acid were purchased from Chengdu Pfiide Biotechnology Co., Ltd., China.

231-MDA-MB-Hpa cell and 4T1 cell are both breast cancer cell line, the former is human-derived and the latter is mouse-derived. 231-MDA-MB-Hpa cell was from Heparinase Sulphate Research Group, Department of Medical Biochemistry, University of Uppsala, Sweden. 4T1 cell was from Shanghai Institute of Cell Biology, Chinese Academy of Sciences, China. High glucose DMEM and foetal bovine serum (FBS) were purchased from Gibco Company, USA. 0.25% trypsin was purchase from Hangzhou Gino Biomedical Technology Co., Ltd,China. Penicillin Streptomycin Solution was purchased from Shanghai Biyuntian Biotechnology Co., Ltd,China. PBS was purchased from Hyclone Company, USA. 25mm²/75mm² Culture bottle, 96 well plate, 5ml/10ml/15ml centrifugal tube, 2ml cryogenic tube were purchased from Corning Company,USA. 0.22 μm filter membrane were purchased from Millipore Company, USA. 10ul/100ul/1000ul pipette tips were purchased from Axygen Company, USA. The proliferation and migration of 4T1 was tested on IncuCyte ZOOM(Essen Bioscience, USA). 231-MDA-MB-Hpa cells were GFP labeled and the proliferation was tested on fluorescence channel on SYNERGY H1 microplate reader(BioTek,USA). While the migration was tested on IncuCyte ZOOM(Essen Bioscience, USA).

According to the ingredients of SH identified by HPLC, Canonical SMILES for each ingredient was matched with PubChem^[11](<https://pubchem.ncbi.nlm.nih.gov/>),with which as ingredient ID, corresponding targets were predicted in Swiss Target Prediction ^[12](<http://www.swisstargetprediction.ch/>) database and SEA^[13] (<http://sea.bkslab.org/>) databases respectively. The screening rules are possibility (> 0.6) for Swiss Target Prediction or Max TC (> 0.6) for SEA. Significant breast cancer target genes were obtained from Therapeutic Target Disease^[14] (TTD, <https://db.idrblab.org/ttd/>), Drug Bank^[15](<https://www.drugbank.ca/>), Disease Gene NET^[16] (DisGeNET, <http://www.disgenet.org/web/DisGeNET/menu/home>) and Gene Association Database (GAD, <https://geneticassociationdb.nih.gov/>). The intersection genes of SH and breast cancer were mapped by Venn Diagram and visualized by Cytoscape3.2.1^[17], after which, protein-protein internetwork (PPI) network of shared genes was constructed with String Database^[18](<https://string-db.org/cgi/input.pl?sessionId=PGNpo2jdjXVs>).Kyoto encyclopaedia of genes and genomes (KEGG) functional annotation clusters were acquired from String database. To visualize PPI network with Cytoscape3.2.1 and top 30 pathways using bubble diagram with omic share(<http://omicshare.com/>) online annotation tool.

Results

Form evolution of SH

In this experiment, 2400ml SH decoction were made of 800g sculellaria barbata and hedyotis diffusa with a ratio of 1:1, then 480ml decoction were made into 13.25g lyophilized powder, the production rate was 8.28%. 100mg/ml mother liquor was formulated with deionized water and kept at -20°C for later cell experiments. In the process of making lyophilized powder of SH, it took 72hours to mainly finish three steps: freezing, main drying and final drying. At least 10°C lower than eutectic point was needed before the start of the process, the eutectic point of SH was detected between -30°C and -40°C in pre-experiment, so -50°C was set as a start temperature. It is considered that lyophilized powder successfully produced when the resistivity is above 95%. Detection diagram of the whole process is as Figure 2.

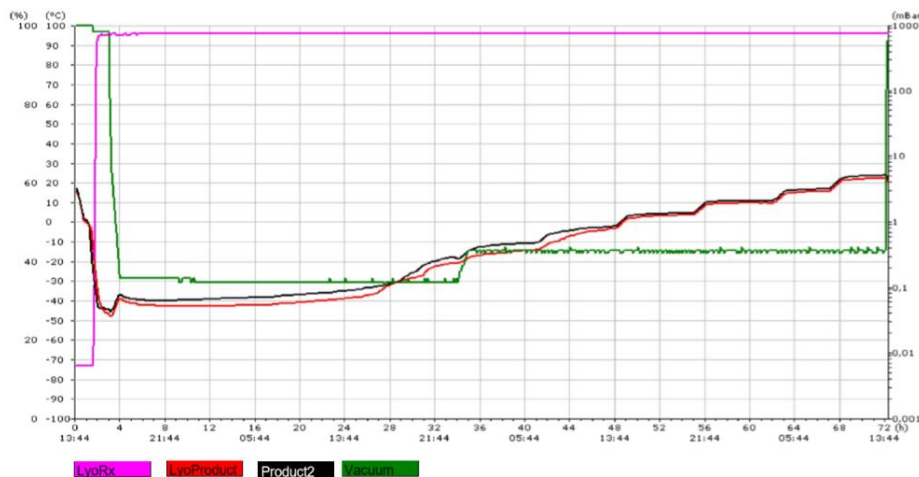


Figure 2 Formation process of lyophilized powder

SH lyophilized powder inhibits breast cancer cells proliferation and migration in vitro

All cells were cultured at 37 °C in a humidified atmosphere containing 5% CO₂. Cells in the exponential phase of growth were used for all experiments.

For the proliferation of mouse-derived breast cancer cell 4T1 with 96-well plate, PBS was filled the edge wells of the plate to keep the microenvironment moist, 2000 cells were seeded in every well of the 96-well plate, from line B to G, from row 2 to 11. The SH concentrations were 0mg/ml, 0.5mg/ml, 1mg/ml, 2mg/ml, 4mg/ml from row 2 to 6, and the same concentration from row 7 to 11. Each column was added with the same SH concentration. The proliferation was tested on Incu-Cyte ZOOM, it took pictures of fixed vision every 4 hours, the Y-axis showed the percentage of the confluence area of cells in the visual field, the X-axis showed the time point. By 60 hours, the confluence of cells in the visual field was up to 99%, meaning that the proliferation of 4T1 cell was limited. For row 6 and row 11, cells with concentration of 4mg/ml showed anomalous data, the results are presented as Figure 3-1. The values of detected percentage of the confluence area with time are presented as Table1-1, corresponding inhibition rate are presented as Table1-2. For cell scratch testing migration of mouse-derived breast cancer cell 4T1 with 96-well plate, PBS was filled the edge wells of the plate to keep the microenvironment moist, 6×10^4 cells were seeded in every well of the 96-well plate, from line B to G, from row 2 to 11. The SH concentrations were 0mg/ml, 0.5mg/ml, 1mg/ml, 2mg/ml, 4mg/ml from row 2 to 6, each column was added with the same SH concentration. The migration was tested on Incu-Cyte ZOOM, the images of migration of 4T1 were taken every 2 hours, after picking out clear and typical images, the results are presented as Figure 3-2

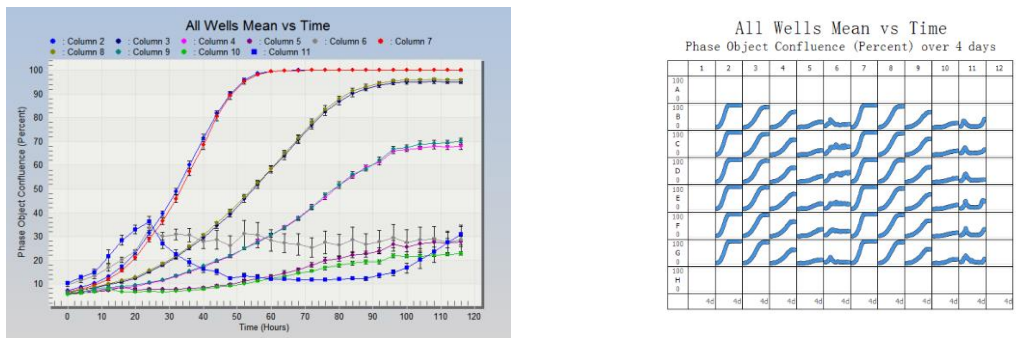


Figure 3-1a. All wells mean vs time grouped by column Figure 3-1b. All wells mean vs time

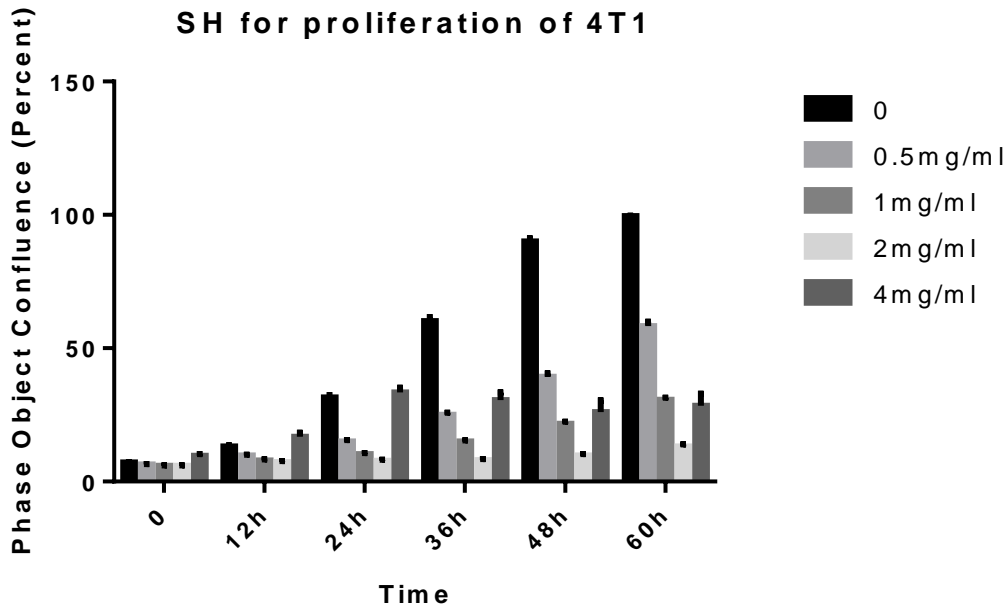


Figure 3-1c. All wells mean vs time grouped by column

Table 1-1. Mean phase object confluence (Percent) grouped by concentration

Confluence (Percent)	0mg/ml		0.5mg/ml		1mg/ml		2mg/ml	
	Mean	SD	Mean	SD	Mean	SD	Mean	SD
0	7.168746	0.174641	6.408026	0.160338	5.909254	0.214415	5.924113	0.175729
12h	13.198900	0.335550	9.789723	0.281281	7.985037	0.265762	7.357464	0.343418
24h	31.500640	0.938027	15.088650	0.496081	10.322470	0.318430	7.872883	0.366319
36h	60.192260	1.515052	25.123370	0.750464	15.021810	0.472186	8.078370	0.376362
48h	90.054750	1.093694	39.358920	1.166853	21.644630	0.755213	9.827250	0.531814
60h	99.557500	0.187575	58.310380	1.566535	30.626970	0.764860	13.236120	0.669873

Table 1-2. Inhibition rate for SH on 4T1

IR	0.5mg/ml	1mg/ml	2mg/ml
0	10.61%	17.57%	17.36%
12h	25.83%	39.50%	44.26%
24h	52.10%	67.23%	75.01%
36h	58.26%	75.04%	86.58%
48h	56.29%	75.97%	89.09%
60h	41.43%	69.24%	86.71%

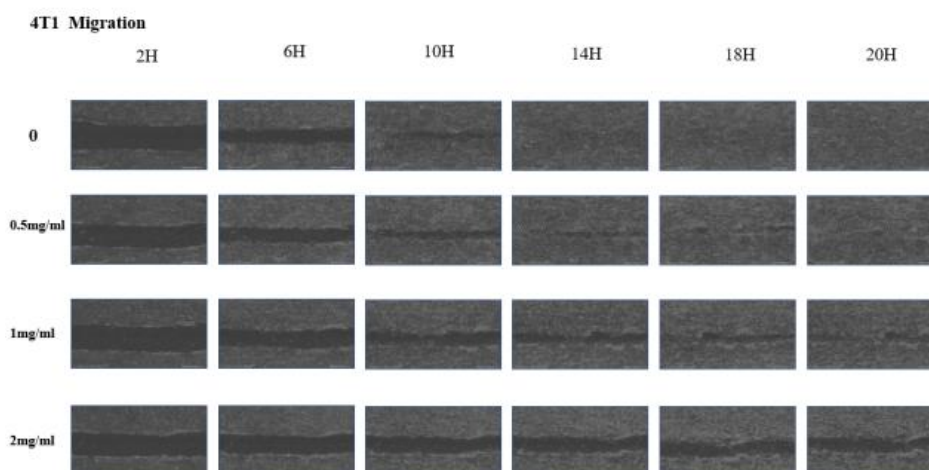


Figure 3-2. Pictures for the migration of SH on 4T1

For the proliferation of human-derived breast cancer cell 231-MDA-MB-Hpa with 96-well plate, PBS was filled the edge wells of the plate to keep the microenvironment moist, 2000 cells were seeded from line B to G, from row 2 to 11. The SH concentrations were 0mg/ml, 0.25mg/ml, 0.5mg/ml, 1mg/ml, 2mg/ml, from row 2 to 6, and the same concentration from row 7 to 11. Each column was added with the same SH concentration. Hpa cells were GFP labelled and the proliferation was tested on fluorescence channel on SYNERGY H1 microplate reader. The Y-axis showed optical density (OD) of GFP, the X-axis showed the time point. For row 2 and row 7, cells with concentration of 0.25mg/ml showed almost the same growth trend with 0mg/ml. the results are presented as Figure 4-1. The values of detected OD of GFP with time are presented as Table2-1, corresponding inhibition rate are presented as Table2-2. For cell scratch testing migration of human-derived breast cancer cell 231-MDA-MB-Hpa with 96-well plate, PBS was filled the edge wells of the plate to keep the microenvironment moist, 6*10⁴ cells were seeded in every well of the 96-well plate, from line B to G, from row 2 to 11. The concentrations were 0mg/ml, 0.5mg/ml, 1mg/ml, 2mg/ml from row 2 to

5, each column was added with the same SH concentration. The migration test was tested on Incu-Cyte ZOOM, the Y-axis showed the percentage of the confluence area of cells in the visual field, the X-axis showed the time point. The images of migration of 4T1 were taken every 2 hours, after picking out clear and typical images, the results are presented as Figure 4-2.

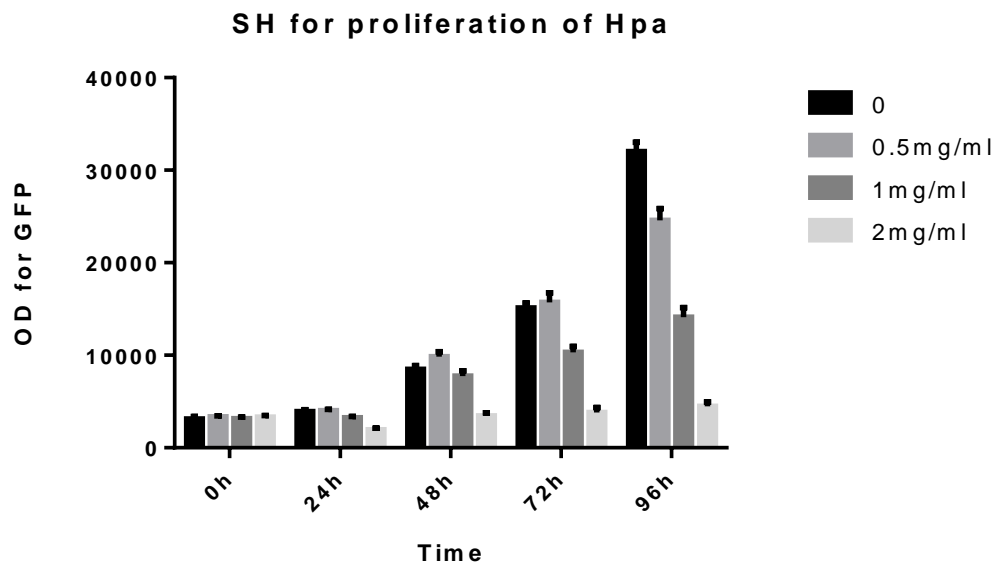


Figure 4-1. All wells mean vs time grouped by column

Table 2-1. Mean GFP OD grouped by concentration

GFP OD	0mg/ml		0.5mg/ml		1mg/ml		2mg/ml	
	Mean	SD	Mean	SD	Mean	SD	Mean	SD
0h	3126.667	246.8025	3341.167	114.6986	3159.667	166.3679	3306.333	167.8102
24h	3908.333	212.3268	4018.000	120.2664	3266.500	132.3174	1945.000	182.0824
48h	8477.000	411.8495	9858.167	510.9088	7761.667	568.9811	3435.333	343.6083
72h	15128.600	525.0093	15714.800	1032.168	10317.200	618.7982	3820.500	519.2012
96h	32018.600	998.5731	24588.800	1266.341	14128.000	1007.305	4485.167	476.5096

Table 2-2. Inhibition rate for SH on 4T1

IR	0.5mg/ml	1mg/ml	2mg/ml
24h	-6.86%	-1.06%	-5.75%
48h	-2.81%	16.42%	50.23%
72h	-16.29%	8.44%	59.47%
96h	-3.87%	31.80%	74.75%

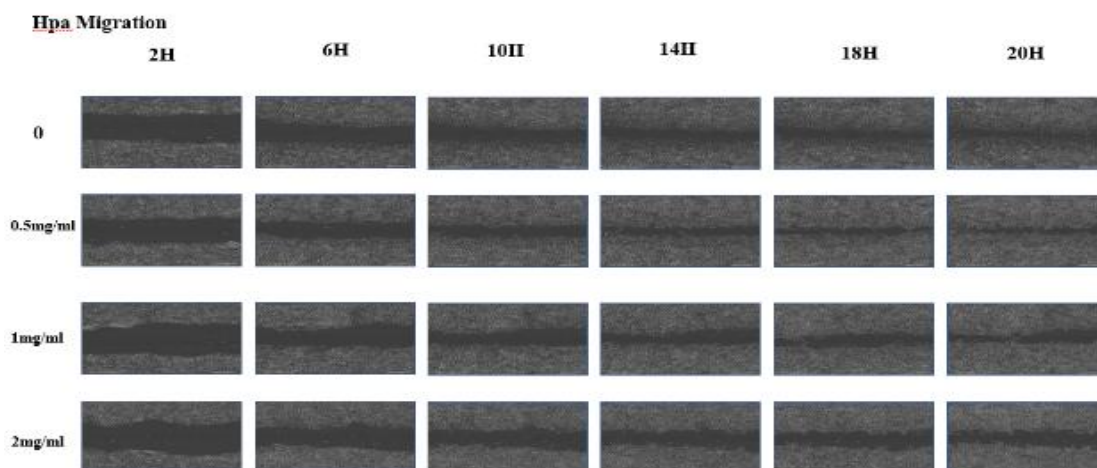


Figure 4-2. Pictures for the migration of SH on Hpa

High Performance Liquid Chromatography and Ingredient Identification.

High performance liquid chromatography (HPLC) was used to identify the main chemical constituents of HS. 100mg Lyophilized powder of SH dissolved in 8 ml 50% methanol solution, ultrasonic vibration for 10 minutes, kept still for 5mins, then another ultrasonic vibration for 10 minutes, kept still for 5mins, 3000r/min centrifugation for 5 minutes, take the supernatant, filtered with 0.22um membrane dilution for testing. The extracts of *Hedyotis diffusa* and *Scutellaria barbata* were analysed and their total ion flow charts under positive and negative ion modes were obtained. According to the retention time, high resolution precise molecular weight and MSn multi-level fragment information obtained by LC-MS, and combined with the extraction of ion flow chart and standard product information, Scifinder database and related literature, 75 ingredients were identified, as shown in Figure 5-1. Among them, 53 ingredients were identified under positive ion mode, 34 ingredients were identified under negative ion mode, 12 shared ingredients were identified by both positive and negative ions, as shown in Figure 5-2. The 75 chemical constituents identified included 43 flavonoids, 9 terpenoids, 9 phenolic acids, 6 alkaloids, 3 coumarins or lignans, 2 anthraquinones and 3 other compounds, as shown in Figure 5-3. Details are listed in Table 3 and 4.

Table 3 Main chemical constituents in positive ion identification of extracts from SH

Peak No.	tR/min	Molecular formula	Measured value m/z	Two level debris (MS/MS)	Possible Ingredient
1	12.39	C ₁₅ H ₁₀ O ₅	271.06010	152.91;229.08;271.12;144.92	Baicalein
2	18.29	C ₁₅ H ₁₀ O ₅	271.06010	152.81;229.08;271.03;144.92	Apigenin
3	11.13	C ₁₅ H ₁₀ O ₆	287.05501	152.84;241.07;168.93; 118.90	Scutellarein
4	12.01	C ₁₅ H ₁₀ O ₆	287.05501	269.00;240.97;168.79;118.88	Isoscutellarein
5	14.74	C ₁₅ H ₁₀ O ₆	287.05501	269.05;241.07;168.88;118.91;287.1	5,7,2',5'-Tetrahydroxyflavone
6	16.36	C ₁₅ H ₁₀ O ₆	287.05501	152.83;287.05;241.01;160.97;269.1	5,7,2',6'-Tetrahydroxyflavone
7	12.04	C ₂₁ H ₁₈ O ₁₂	463.08710	287.08;301.13	Scutellarein 7-glucuronide
8	15.06	C ₂₁ H ₁₈ O ₁₂	463.08710	287.08;288.18	5,6,7,2'-Tetrahydroxyflavone 7-glucuronide
9	10.31	C ₁₅ H ₁₀ O ₇	303.04993	256.97;229.00;164.88;285.03;246.99	Viscidulin I
10	13.07	C ₁₅ H ₁₀ O ₇	303.04993	257.01;229.02;164.92;285.07;246.97	3,5,7,2',5'-Pentahydroxyflavone
11	13.68	C ₂₁ H ₁₈ O ₁₁	447.09218	270.96;260.20	Baicalin
12	13.76	C ₂₁ H ₂₀ O ₁₁	449.10783	271.00;285.08	Cinaroside
13	23.98	C ₁₆ H ₁₂ O ₄	269.08083	254.07;223.03;237.00;255.05	Chrysin-5-methylether
14	18.32	C ₁₆ H ₁₂ O ₆	301.07066	286.03;286.99	Hispidulin
15	13.92	C ₂₂ H ₂₀ O ₁₂	477.10275	301.12;339.33	Hispidulin 7-O-beta-glucuronide
16	16.5	C ₁₇ H ₁₄ O ₆	315.08631	302.02;303.08	Skullcapflavone I
17	24.31	C ₁₇ H ₁₄ O ₆	315.08631	299.23;281.13;239.20;257.13;271.10	5,7-Dihydroxy-8,2'-dimethoxyflavone
18	24.39	C ₁₇ H ₁₄ O ₆	315.08631	295.18;267.09;108.84;285.13	5,8-Dihydroxy-6,7-dimethoxyflavone

19	26.94	C ₁₈ H ₁₆ O ₆	329.10196	296.02;314.05;297.11;315.09	7-Hydroxy-5,8,2'-trimethoxyflavone
20	22.01	C ₁₈ H ₁₆ O ₇	345.09687	330.08;312.13;331.22;313.08	Tenaxin I
21	24.80	C ₁₉ H ₁₈ O ₇	359.11252	326.10;344.12;327.07;345.14	Altisin
22	21.83	C ₁₉ H ₁₈ O ₈	375.10744	342.08;360.11;343.12;361.25;314.08	Skullcapflavone II
23	11.45	C ₂₆ H ₂₈ O ₁₄	565.15518	547.23;433.31;403.10;521.30;548.40	Isoschaftoside
24	12.39	C ₁₆ H ₁₄ O ₄	271.09648	152.91;229.08;271.12;144.92	(-)-Alpinetin
25	11.84	C ₁₅ H ₁₂ O ₆	289.07066	168.85;146.87;188.86	Eriodictyol
26	12.62	C ₁₅ H ₁₂ O ₆	289.07066	168.86;146.96;194.98;188.98	Carthamidin
27	14.96	C ₁₅ H ₁₂ O ₆	289.07066	168.95;146.84;188.93	Isocarthamidin
28	14.32	C ₁₆ H ₁₄ O ₆	303.08631	182.92;146.88;167.96	5,7,4'-Trihydroxy-6-methoxyflavanone
29	18.20	C ₁₆ H ₁₄ O ₆	303.08631	182.95;146.86;167.85	Scutamoenin
30	13.79	C ₁₅ H ₁₂ O ₅	273.07575	152.80;146.83;178.88	Dihydrobaicalein
31	10.31	C ₁₅ H ₁₂ O ₇	305.06557	256.97;229.00;164.88;285.03;246.99	3,5,7,2',5'-Pentahydroxyflavanone
32	13.07	C ₁₅ H ₁₂ O ₇	305.06557	257.01;229.02;164.92;285.07;246.97	3,5,7,2',6'-Pentahydroxyflavanone
33	18.07	C ₂₂ H ₃₀ O ₆	391.21151	373.27;345.20;251.10	Jodrellin A
34	20.59	C ₂₂ H ₃₀ O ₆	391.21151	373.25;313.30;331.15;295.32;345.27	Isomers of Jodrellin A
35	21.78	C ₂₂ H ₃₀ O ₆	391.21151	331.24;313.20;275.13;295.09;247.20	Isomers of Jodrellin A
36	24.80	C ₂₂ H ₃₀ O ₆	391.21151	331.13;313.08;295.20;257.20;271.26	Isomers of Jodrellin A
37	9.43	C ₂₂ H ₃₂ O ₇	409.22207	229.12;202.95;247.05	11-Episcutecolumnin C
38	23.34	C ₂₂ H ₃₂ O ₈	425.21699	407.15;274.08;408.32	Scutalbin C
39	11.04	C ₁₀ H ₁₀ O ₃	179.07027	144.91;116.92	p-MCA
40	11.08	C ₁₁ H ₁₄ O ₂	179.10665	144.88;148.96	Methyleugenol
41	12.92	C ₁₀ H ₁₀ O ₂	163.07535	144.92;117.00;126.90	p-Hydroxybenzalacetone
42	12.95	C ₁₀ H ₁₂ O ₂	165.09100	144.88;116.96;134.96;126.87	3'-Hydroxyanethole
43	25.97	C ₃₀ H ₃₇ NO ₉	556.25411	514.32;313.17;235.03;295.11	Scutebarbatine F
44	26.70	C ₃₂ H ₃₄ N ₂ O ₇	559.24387	436.23;295.26;313.19;249.22	Scutebarbatine A
45	20.10	C ₂₆ H ₃₃ NO ₇	472.23297	455.21;454.25;313.16;249.06;389.30	Scutebarbatine G
46	28.20	C ₂₈ H ₃₃ NO ₇	496.23297	295.21;313.13;271.03266.94;253.30	Scutebarbatine K
47	20.52	C ₃₂ H ₃₄ N ₂ O ₈	575.23879	515.32;557.34;516.25;353.14	7-O-Nicotinoylscutebarbatine H
48	20.33	C ₃₂ H ₃₄ N ₂ O ₈	575.23879	515.32;557.34;516.25;353.14	Isomers of 7-O-Nicotinoylscutebarbatine H
49	6.90	C ₁₀ H ₈ O ₄	193.04954	146.89;174.95;165.02;148.90	Scopoletin
50	2.50	C ₂₀ H ₁₈ O ₆	355.11761	192.95;324.08;325.12;184.98;323.32	Capitellataquinone A
51	24.07	C ₁₅ H ₁₀ O ₃	239.07027	210.96;183.00;193.03;164.98	2-hydroxy-3-methylanthraquinone
52	13.98	C ₃₂ H ₄₆ O ₁₁	607.31128	495.18;363.16;496.18	Scupontin B
53	15.91	C ₃₂ H ₄₆ O ₁₁	607.31128	496.19;363.19	Isomers of Scupontin B

Table 4 Main chemical constituents in anion identification of extracts from SH

Peak No.	tR/min	Molecular formula	Measured value m/z	Two level debris (MS/MS)	Possible Ingredient
1	12.44	C ₁₅ H ₁₀ O ₅	269.04555	224.97; 148.92; 183.08; 197.03	Baicalein
2	18.31	C ₁₅ H ₁₀ O ₅	269.04555	225.09; 148.94; 200.98; 182.96	Apigenin
3	13.74	C ₁₅ H ₁₀ O ₅	269.04555	225.04; 148.92; 182.94; 196.92	5,7,2'-Trihydroxyflavone
4	11.06	C ₁₅ H ₁₀ O ₆	285.04046	266.93; 238.93; 185.02; 164.88; 213.04	Scutellarein
5	12.10	C ₁₅ H ₁₀ O ₆	285.04046	241.08; 212.98; 257.06; 266.95	Isoscutellarein
6	16.40	C ₁₅ H ₁₀ O ₆	285.04046	240.98; 198.91; 174.96; 216.89; 150.84	5,7,2',6'-Tetrahydroxyflavone
7	12.21	C ₂₁ H ₁₈ O ₁₂	461.07255	285.03; 357.20; 327.13	Scutellarein 7-glucuronide
8	15.10	C ₂₁ H ₁₈ O ₁₂	461.07255	285.08; 299.17	5,6,7,2'-Tetrahydroxyflavone 7-glucuronide
9	10.74	C ₁₅ H ₁₀ O ₇	301.03540	286.04; 181.02; 255.06	Viscidulin I

10	13.35	C ₁₅ H ₁₀ O ₇	301.03540	286.10; 180.95; 207.01	3,5,7,2',5'-Pentahydroxyflavone
11	13.73	C ₂₁ H ₁₈ O ₁₁	445.07763	268.97; 175.01	Baicalin
12	13.80	C ₂₁ H ₂₀ O ₁₁	447.09328	271.05; 174.92; 285.05	Cinaroside
13	11.17	C ₂₁ H ₂₀ O ₁₁	447.09328	271.06; 175.06; 327.09	Dihydrobaicalein 7-O-glucuronide
14	11.8	C ₂₁ H ₂₀ O ₁₂	463.08820	286.97; 269.09; 174.98	3,5,7,2',6'-Pentahydroxyflavone 2'-glucoside
15	12.66	C ₂₁ H ₂₀ O ₁₂	463.08820	287.18; 445.24; 401.39	Isomers of 3,5,7,2',6'-Pentahydroxyflavone 2'-glucoside
16	18.07	C ₁₆ H ₁₂ O ₄	267.06628	252.02; 239.11; 223.11	Chrysin-5-methylether
17	24.39	C ₁₆ H ₁₂ O ₄	267.06628	223.25; 249.14; 167.08; 193.13	Isomers of Chrysin-5-methylether
18	12.43	C ₂₁ H ₂₀ O ₁₀	431.09837	269.08; 311.17	Isovitexin
19	13.8	C ₂₂ H ₂₂ O ₁₀	445.11402	269.00; 286.90	Baicalein 6-methyl ether 7-glucoside
20	9.56	C ₂₃ H ₂₂ O ₁₁	473.10893	251.04; 224.83; 268.98; 455.30; 413.22	7-Hydroxy-5,8-dimethoxyflavone 7-glucuronide
21	17.73	C ₂₂ H ₂₀ O ₁₁	459.09328	333.20; 427.25; 451.32	Baicalein 6-methyl ether 7-glucuronide
22	1.86	C ₁₆ H ₂₀ O ₁₀	371.09793	353.19; 208.91; 191.08; 164.93; 134.92	Deacetyl asperuloside
23	10.10	C ₁₆ H ₂₀ O ₁₀	371.09793	248.9; 231.04	Isomers of Deacetyl asperuloside
24	16.00	C ₃₁ H ₄₀ O ₁₅	651.22944	475.33; 505.22; 457.29; 192.97	Isomartynoside
25	39.72	C ₃₀ H ₄₈ O ₃	455.35307	407.55; 386.86; 318.75	Ursolic acid
26	4.26	C ₉ H ₈ O ₃	163.04006	118.95; 147.69	trans-p-Coumaric acid
27	7.60	C ₉ H ₈ O ₃	163.04006	118.92; 134.95	Isomers of trans-p-Coumaric acid
28	10.89	C ₉ H ₈ O ₃	163.04006	118.91; 134.96	Isomers of trans-p-Coumaric acid
29	8.25	C ₉ H ₈ O ₂	147.04515	118.98; 102.93; 90.89	cinnamic acid
30	7.47	C ₇ H ₆ O ₂	121.02950	92.81; 120.81; 105.58	HBA
31	9.88	C ₈ H ₈ O	119.05024	118.88; 92.79	succinic acid
32	7.78	C ₉ H ₈ O ₄	179.03498	134.87; 150.93	Caffeic acid
33	3.95	C ₉ H ₈ O ₄	179.03498	134.81; 146.91	Isomers of Caffeic acid
34	14.02	C ₃₁ H ₃₆ O ₁₁	583.21848	421.23; 289.17; 451.34	Hedyotol C

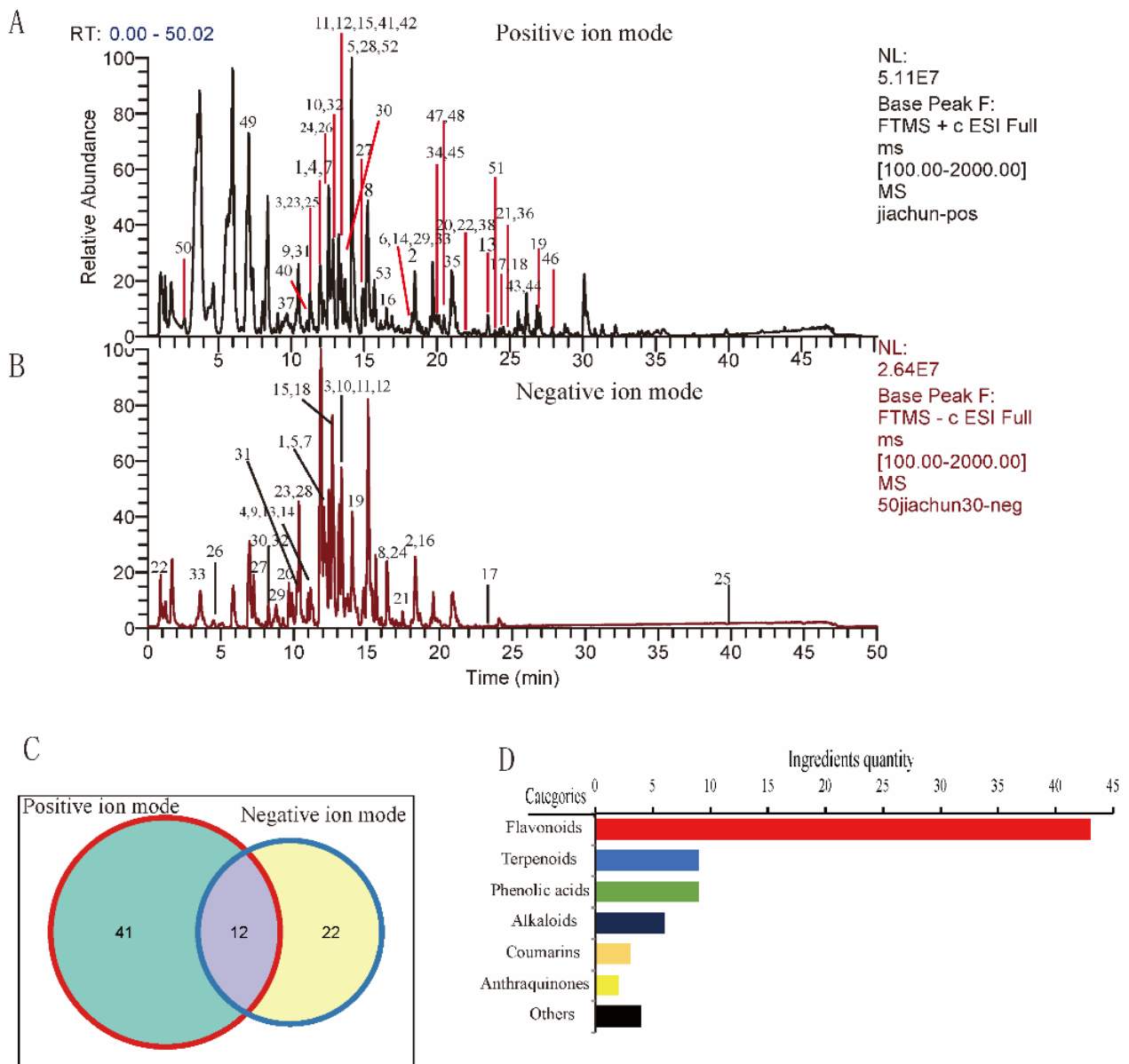


Figure 5 Main ingredients and categories

Target genes collection for SH and breast cancer

After searching and matching, 55 of 75 ingredients matched SMILES codes, while 8 ingredients that did not find matching SMILES codes, what worth noting is that SMILES represents two-dimensional ID and isomers share one SMILES code (Supplement table 1) . According to the screening rules mentioned before, 137 target genes in Swiss Target Prediction database and 106 target genes in SEA database were obtained, and 180 target genes were retained after cutting off duplicate values (Supplement table 2-4) .

A total of 1305 target genes were found for breast cancer candidate genes. 68 breast cancer targets from TTD, 198 from Drugbank, 329 from DisGeNET and 890 from GAD(Supplement 5). Targets of several databases intersect as shown in Figure 6.

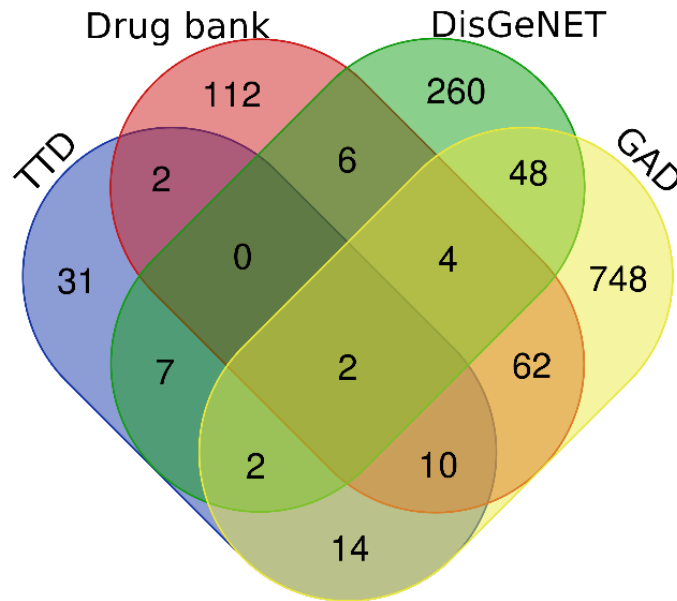


Figure 6 Venn for breast cancer target genes from different databases

Target genes mapping and network construction

Target genes were mapped for SH and breast cancer as shown in Figure 7. The PPI network of shared genes was constructed by Cytoscape3.2.1 on the basis on data from String database, as shown in Figure 8. Parameters were calculated by Network Analyzer shown in Table 5. Degree means the number of nodes directly interacting with some one node, the larger it is, the more biological functions the node participates in; Betweenness of one node means the proportion of all the shortest paths linked to this node in the network, the larger it is, the more important the node is; Closeness centrality means and average shortest path length also weigh a node in the network, the smaller they are, the more important for the node.

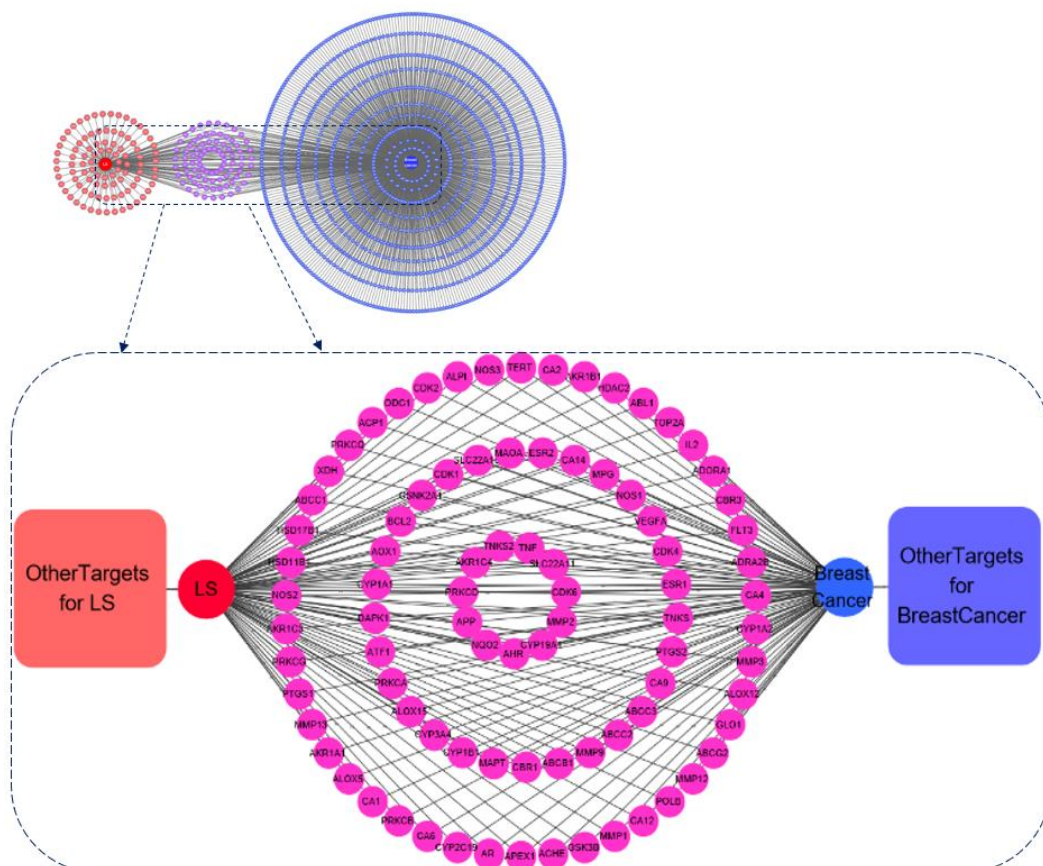


Figure 7 Target genes mapping for SH and breast cancer

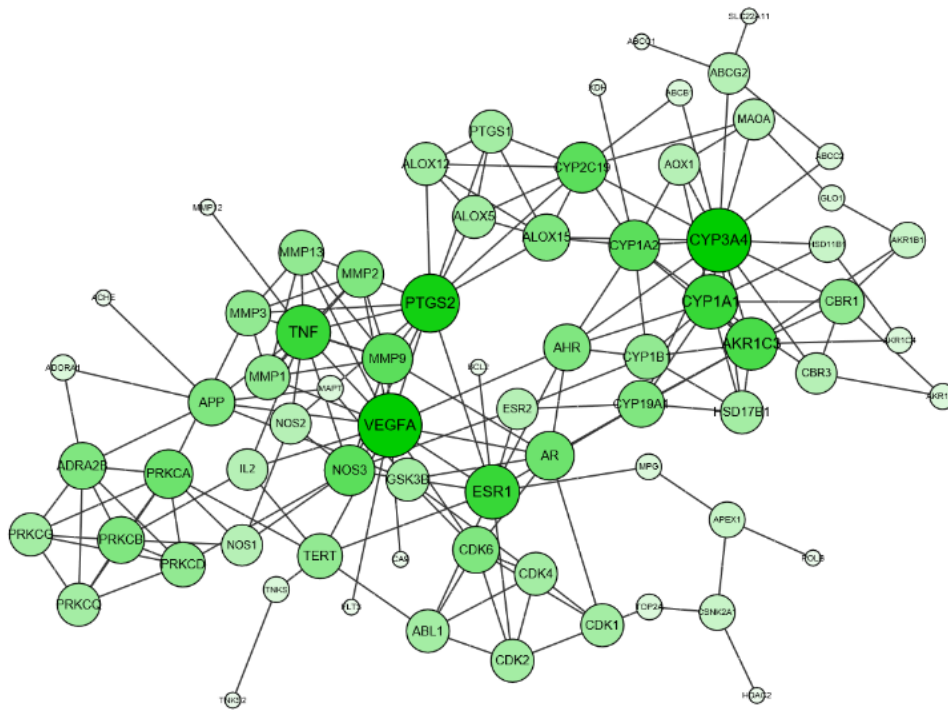


Figure 8. PPI network of shared target genes

Table 5 Parameters of genes in PPI network

Gene Name	Degree	Betweenness centrality	Closeness centrality	Average shortest path length
CYP3A4	16	0.21	0.37	2.69
VEGFA	16	0.25	0.45	2.23
PTGS2	13	0.16	0.41	2.45
CYP1A1	11	0.04	0.35	2.89
ESR1	11	0.22	0.43	2.32
TNF	11	0.05	0.36	2.76
AKR1C3	10	0.09	0.36	2.75
CYP1A2	9	0.04	0.35	2.85
CYP2C19	9	0.06	0.36	2.76
MMP9	9	0.02	0.37	2.69
NOS3	9	0.08	0.38	2.65
AR	8	0.13	0.40	2.52
PRKCA	8	0.04	0.31	3.27
ADRA2B	7	0.02	0.28	3.59
AHR	7	0.15	0.41	2.42
ALOX15	7	0.03	0.36	2.80
APP	7	0.09	0.34	2.92
CDK6	7	0.03	0.35	2.85
CYP19A1	7	0.08	0.39	2.59
MMP2	7	0.00	0.34	2.93
PRKCB	7	0.01	0.28	3.63
CBR1	6	0.02	0.29	3.39
CYP1B1	6	0.01	0.34	2.97
MMP1	6	0.00	0.33	3.06
MMP13	6	0.00	0.33	3.06
MMP3	6	0.02	0.33	3.03
PRKCD	6	0.02	0.30	3.34
TERT	6	0.09	0.36	2.79
ABL1	5	0.01	0.33	3.03
ALOX12	5	0.00	0.32	3.08
ALOX5	5	0.00	0.32	3.08

CDK1	5	0.06	0.31	3.24
CDK2	5	0.01	0.32	3.10
CDK4	5	0.01	0.29	3.49
GSK3B	5	0.03	0.32	3.15
HSD17B1	5	0.00	0.31	3.20
PRKCG	5	0.00	0.25	4.04
PRKCQ	5	0.00	0.25	4.04
PTGS1	5	0.00	0.32	3.08
ABCG2	4	0.06	0.28	3.61
AOX1	4	0.00	0.28	3.59
CBR3	4	0.01	0.28	3.59
ESR2	4	0.02	0.36	2.80
IL2	4	0.02	0.34	2.97
MAOA	4	0.02	0.30	3.38
NOS1	4	0.00	0.29	3.44
NOS2	4	0.00	0.32	3.13
AKR1B1	3	0.01	0.27	3.65
APEX1	3	0.05	0.25	4.04
CSNK2A1	3	0.03	0.21	4.70
HSD11B1	3	0.00	0.28	3.62
ABCB1	2	0.00	0.29	3.44
ABCC2	2	0.00	0.28	3.63
ADORA1	2	0.00	0.26	3.79
AKR1A1	2	0.00	0.23	4.37
AKR1C4	2	0.00	0.27	3.70
GLO1	2	0.00	0.24	4.14
MAPT	2	0.00	0.27	3.65
MPG	2	0.08	0.31	3.18
TNKS	2	0.03	0.27	3.75
TOP2A	2	0.03	0.24	4.10
ABCC1	1	0.00	0.22	4.59
ACHE	1	0.00	0.26	3.90
BCL2	1	0.00	0.30	3.31
CA9	1	0.00	0.31	3.21
FLT3	1	0.00	0.31	3.21
HDAC2	1	0.00	0.18	5.69
MMP12	1	0.00	0.27	3.75
POLB	1	0.00	0.20	5.03
SLC22A11	1	0.00	0.22	4.59
TNKS2	1	0.00	0.21	4.73

Pathway enrichment and analysis

Kyoto Encyclopedia of Genes and Genomes (KEGG) functional annotation clusters were acquired from String database (Supplement table 6). To visualize top 30 pathways with bubble diagram (Figure 9).

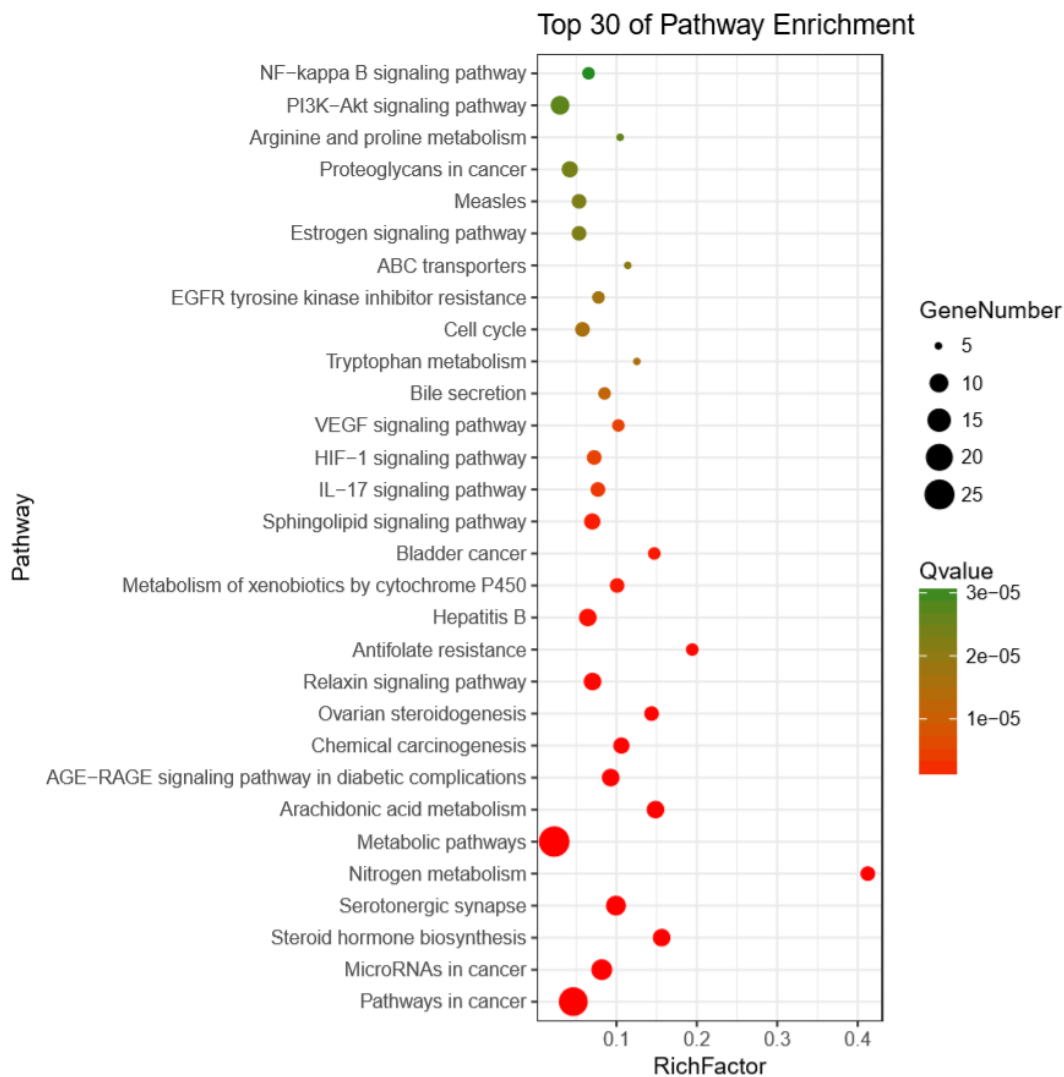


Figure 9 Top 30 KEGG pathways

Discussion:

This study evaluated the efficacy of SH lyophilized powder on human-derived and mouse-derived breast cancer cells *in vitro*. Besides, some key genes and many potential pathways were found through PPI network construction of intersection genes. Key genes like BCL-2 is one of the most important oncogenes in apoptotic research, similarly, 7 cell cycle related genes were mapped ABL1, CDK1, CDK2, CDK4, CDK6, GSK3B, HDAC2, as we all know that cell apoptosis and cell cycle are the most common drug effects, which can be considered as the preferred experiment validation. Some enriched pathways are widely discussed in cancer. Studies have shown that NF-KB can play an anti-apoptotic role in breast cancer, and it is related to the antibody of estrogen and progesterone and the expression of HER-2 gene in breast cancer^[19]. In addition, relevant studies have confirmed that^[20-22] in some kinds of breast cancer cells, sustained activation of NF-KB was found. By inhibiting the activation of NF-KB, the sensitivity of breast cancer cells to anthracycline drugs could be reversed, further, migration and invasion of TNF-alpha-mediated breast cancer cells could be inhibited. Vascular endothelial growth factor (VEGF) is a highly sensitive marker of malignant tumours^[23, 24]. It not only promotes the formation of blood vessels in breast tumours, but also promotes the metastasis of tumours through lymphatic channels^[25]. Micro RNA in cancer is getting widely studied and discussed in recent years, it plays a major role in gene expression modulation and controlling major pathways. Dysregulation in micro RNA expression is associated with cancers^[26, 27] and can act as promotor (oncomiR) or suppressors of tumorigenesis (antioncomiR)^[28], miRNAs have been dysregulated in breast cancer as shown by profiling breast tissues from healthy individuals and those from breast cancer patients^[29], they appear to be ideal biomarkers for diagnosis, follow-up, and prognosis prediction of cancer patients^[30].

About SH form evolution, we all know that Chinese medicine come from herbs, process into slices and taken as decoction, however, due to too much large particles in the decoction, making it hard to be filtrated by 0.22um membrane. Derived from SH decoction and closest to the original state of TCM decoction, lyophilized powder is an indispensable form for cell experiments *in vitro*.

Target genes in TTD and Drug Bank were drug-validated, target genes in DisGeNET came from published literatures. GAD is a relatively primitive database with comprehensive content, which can complement the above verified targets. As figure 9 shows: several databases can not cover each other for the main direction each database is different, as network discussion, as comprehensive as possible target genes are necessary, so we took sum aggregate of these four databases for mapping and further discussion.

There are several limitations of the study: (i) It is unclear the efficiency proportion and possible side effects of each ingredient. (ii) There were only cell experiments for efficacy evaluation. (iii) Different target prediction and enrichment tools presented different results and even with visualized results of pathways, we have no idea of activation or inhibition effects, so further validations are essential. The efficacy validation of SH on nude mice model of triple-negative breast cancer and key proteins experimental validations such as cell cycle and apoptosis, EGFR pathway are two main parts of our present work. After that, precise efficacy of each ingredient is a long journey in the future.

In conclusion, SH plays an efficacy enhancing role in the treatment of breast cancer in accordance with detoxification principle in TCM. To our knowledge, Chinese medicine compatibilities sharing the same treating principle have the same or similar functions with different herbs, but the curative effects are imprecise from one herb to another for species diversity, better prescriptions with more definite efficacy will be optimized with the visualization process and validation of active ingredients, targets and pathways by network pharmacology.

References:

- [1] Swarup AB, Barrett W, Jazieh AR. (2006). The use of complementary and alternative medicine by cancer patients undergoing radiation therapy. *Am J Clin Oncol* 2006; 29(5): 468-473.
- [2] Hyodo I, Amano N, Eguchi K, Narabayashi M, Imanishi J, Hirai M, Nakano T, Takashima S. (2005). Nationwide survey on complementary and alternative medicine in cancer patients in Japan. *J Clin Oncol* 2005; 23(12): 2645-2654.
- [3] Evans MA, Shaw AR, Sharp DJ, Thompson EA, Falk S, Turton P, Thompson T. (2007). Men with cancer: is their use of complementary and alternative medicine a response to needs unmet by conventional care? *Eur J Cancer Care (Engl)* 2007; 16(6): 517-525.
- [4] Yeh YC, Chen HY, Yang SH, Lin YH, Chiu JH, Lin YH, Chen JL. (2014). Hedyotis diffusa Combined with Scutellaria barbata Are the Core Treatment of Chinese Herbal Medicine Used for Breast Cancer Patients: A Population-Based Study. *Evid Based Complement Alternat Med* 2014; 2014: 202378.
- [5] Hopkins AL. Network pharmacology: the next paradigm in drug discovery. (2008). *Nat Chem Biol* 2008; 4(11): 682-690.
- [6] Li S, Zhang B. (2013). Traditional Chinese medicine network pharmacology: theory, methodology and application. *Chin J Nat Med* 2013; 11(2): 110-120.
- [7] Wang N, Yang B, Zhang X, Wang S, Zheng Y, Li X, Liu S, Pan H, Li Y, Huang Z, Zhang F, Wang Z. (2018). Network Pharmacology-Based Validation of Caveolin-1 as a Key Mediator of Ai Du Qing Inhibition of Drug Resistance in Breast Cancer. *Front Pharmacol* 2018; 9: 1106.
- [8] Gao L, Wang XD, Niu YY, Duan DD, Yang X, Hao J, Zhu CH, Chen D, Wang KX, Qin XM, Wu XZ. (2016). Molecular targets of Chinese herbs: a clinical study of hepatoma based on network pharmacology. *Sci Rep* 2016; 6: 24944.
- [9] Yue SJ, Xin LT, Fan YC, Li SJ, Tang YP, Duan JA, Guan HS, Wang CY. (2017). Herb pair Danggui-Honghua: mechanisms underlying blood stasis syndrome by system pharmacology approach. *Sci Rep* 2017; 7: 40318.
- [10] Gao L, Wang KX, Zhou YZ, Fang JS, Qin XM, Du GH. (2018). Uncovering the anticancer mechanism of Compound Kushen Injection against HCC by integrating quantitative analysis, network analysis and experimental validation. *Sci Rep* 2018; 8(1): 624.
- [11] Kim S, Chen J, Cheng T, Gindulyte A, He J, He S, Li Q, Shoemaker BA, Thiessen PA, Yu B, Zaslavsky L, Zhang J, Bolton EE. (2019). PubChem 2019 update: improved access to chemical data. *Nucleic Acids Res* 2019; 47(D1): D1102-D1109.
- [12] Gfeller D, Grosdidier A, Wirth M, Daina A, Michielin O, Zoete V. (2014). SwissTargetPrediction: a web server for target prediction of bioactive small molecules. *Nucleic Acids Res* 2014; 42(Web Server issue): W32-W38.
- [13] Keiser MJ, Roth BL, Armbruster BN, Ernsberger P, Irwin JJ, Shoichet BK. (2007). Relating protein pharmacology by ligand chemistry. *Nat Biotechnol* 2007; 25(2): 197-206.

- [14]Li YH, Yu CY, Li XX, Zhang P, Tang J, Yang Q, Fu T, Zhang X, Cui X, Tu G, Zhang Y, Li S, Yang F, Sun Q, Qin C, Zeng X, Chen Z, Chen YZ, Zhu F. (2018).Therapeutic target database update 2018: enriched resource for facilitating bench-to-clinic research of targeted therapeutics. *Nucleic Acids Res* 2018; 46(D1): D1121-D1127.
- [15]Wishart DS, Feunang YD, Guo AC, Lo EJ, Marcu A, Grant JR, Sajed T, Johnson D, Li C, Sayeeda Z, Assempour N, Iynkkaran I, Liu Y, Maciejewski A, Gale N, Wilson A, Chin L, Cummings R, Le D, Pon A, Knox C, Wilson M. (2018).DrugBank 5.0: a major update to the DrugBank database for 2018. *Nucleic Acids Res* 2018; 46(D1): D1074-D1082.
- [16]Pinero J, Bravo A, Queralt-Rosinach N, Gutierrez-Sacristan A, Deu-Pons J, Centeno E, Garcia-Garcia J, Sanz F, Furlong LI. (2017).DisGeNET: a comprehensive platform integrating information on human disease-associated genes and variants. *Nucleic Acids Res* 2017; 45(D1): D833-D839.
- [17]Shannon P, Markiel A, Ozier O, Baliga NS, Wang JT, Ramage D, Amin N, Schwikowski B, Ideker T. (2003).Cytoscape: a software environment for integrated models of biomolecular interaction networks. *Genome Res* 2003; 13(11): 2498-2504.
- [18]Szkklarczyk D, Gable AL, Lyon D, Junge A, Wyder S, Huerta-Cepas J, Simonovic M, Doncheva NT, Morris JH, Bork P, Jensen LJ, Mering CV. (2019).STRING v11: protein-protein association networks with increased coverage, supporting functional discovery in genome-wide experimental datasets. *Nucleic Acids Res* 2019; 47(D1): D607-D613.
- [19]Biswas DK, Shi Q, Baily S, Strickland I, Ghosh S, Pardee AB, Iglehart JD. (2004).NF-kappa B activation in human breast cancer specimens and its role in cell proliferation and apoptosis. *Proc Natl Acad Sci U S A* 2004; 101(27): 10137-10142.
- [20]Choi YK, Cho SG, Woo SM, Yun YJ, Jo J, Kim W, Shin YC, Ko SG. (2013).Saussurea lappa Clarke-Derived Costunolide Prevents TNF alpha -Induced Breast Cancer Cell Migration and Invasion by Inhibiting NF- kappa B Activity. *Evid Based Complement Alternat Med* 2013; 2013: 936257.
- [21]Zong H, Wang F, Fan QX, Wang LX. (2012).Curcumin inhibits metastatic progression of breast cancer cell through suppression of urokinase-type plasminogen activator by NF-kappa B signaling pathways. *Mol Biol Rep* 2012; 39(4): 4803-4808.
- [22]Connelly L, Barham W, Onishko HM, Sherrill T, Chodosh LA, Blackwell TS, Yull FE. (2011).Inhibition of NF-kappa B activity in mammary epithelium increases tumor latency and decreases tumor burden. *Oncogene* 2011; 30(12): 1402-1412.
- [23]Reiter MJ, Costello JE, Schwoppe RB, Lisanti CJ, Osswald MB. (2015).Review of Commonly Used Serum Tumor Markers and Their Relevance for Image Interpretation. *J Comput Assist Tomogr* 2015; 39(6): 825-834.
- [24]Sharma G, Mirza S, Parshad R, Srivastava A, Gupta SD, Pandya P, Ralhan R. (2011).Clinical significance of Maspin promoter methylation and loss of its protein expression in invasive ductal breast carcinoma: correlation with VEGF-A and MTA1 expression. *Tumour Biol* 2011; 32(1): 23-32.
- [25]Cohen-Kaplan V, Naroditsky I, Zetser A, Ilan N, Vlodavsky I, Doweck I. (2008).Heparanase induces VEGF C and facilitates tumor lymphangiogenesis. *Int J Cancer* 2008; 123(11): 2566-2573.
- [26]Mendell JT, Olson EN. (2012).MicroRNAs in stress signaling and human disease. *Cell* 2012; 148(6): 1172-1187.
- [27]Song S, Ajani JA. (2013).The role of microRNAs in cancers of the upper gastrointestinal tract. *Nat Rev Gastroenterol Hepatol* 2013; 10(2): 109-118.
- [28]Svoronos AA, Engelman DM, Slack FJ. (2016).OncomiR or Tumor Suppressor? The Duplicity of MicroRNAs in Cancer. *Cancer Res* 2016; 76(13): 3666-3670.
- [29]Hamam R, Hamam D, Alsaleh KA, Kassem M, Zaher W, Alfayez M, Aldahmash A, Alajez NM. (2017).Circulating microRNAs in breast cancer: novel diagnostic and prognostic biomarkers. *Cell Death Dis* 2017; 8(9): e3045.
- [30]van Schooneveld E, Wouters MC, Van der Auwera I, Peeters DJ, Wildiers H, Van Dam PA, Vergote I, Vermeulen PB, Dirix LY, Van Laere SJ. (2012).Expression profiling of cancerous and normal breast tissues identifies microRNAs that are differentially expressed in serum from patients with (metastatic) breast cancer and healthy volunteers. *Breast Cancer Res* 2012; 14(1): R34.